ISSN 1063-7850, Technical Physics Letters, 2020, Vol. 46, No. 6, pp. 526–531. © Pleiades Publishing, Ltd., 2020.

Active Tuning of Hybrid Plasmonics in Graphene-Covered Metallic Nanotrench

Noor Uddin[a,c], Qing Yang[b], Guangqing Du[a]*, Feng Chen[a], Huijing Li[a], and Xun Hou[a]**

[a] *Department of Electronic Science and Technology, State Key Laboratory for Manufacturing System Engineering and Key Laboratory of Photonics Technology for Information of Shaanxi Province, School of Electronics and Information Engineering, Xi'an Jiaotong University, Xi'an, 710049 P.R. China*

[b] *School of Mechanical Engineering, Xi'an Jiaotong University, Xi'an, 710049 P.R. China*

[c] *Department of Computer Systems Engineering and Sciences, Balochistan University of Engineering and Technology, Khuzdar, 89100 Pakistan*

**e-mail: guangqingdu@mail.xjtu.edu.cn*

***e-mail: chenfeng@mail.xjtu.edu.cn*

Received September 20, 2019; revised March 2, 2020; accepted March 6, 2020

Abstract—Graphene has recently emerged as a possible platform for integrated optoelectronics and hybrid photonic devices because of its promising electronic and optical characteristics. Here, we propose the active tuning of hybrid plasmonics in intrinsic graphene-based gold rectangle nanotrench by modifying the graphene electron system. We found that the plasmonics response in graphene thicknesses can be unprecedentedly tuned by altering the thickness of thick graphene covering nanotrench geometry. It is explained as the active plasmonics hybridization leading to the tunability of the enhanced *e*-field localized within the graphene-covered metallic nanotrench. This study can be useful for optoelectronic devices based on hybrid graphene structures at IR wavelengths.

Keywords: graphene plasmonics, hybridization, tunabilities, graphene thickness, Fermi levels.

DOI: 10.1134/S1063785020060115

In recent years, graphene has been introduced to the field of plasmonics [1] and offers fresh ways to operate and confine light on the nanoscale. Graphene, a single atomic film of graphite, has fascinated great attention since it was first isolated by mechanical exfoliation in 2004 [2]. Graphene exhibits a thin body, a unique energy band structure, excellent electrical transport properties, high mechanical and thermodynamic strength [2–7], which make it a capable candidate for future nanoelectronic devices. Graphene can be patterned to different periodic plasmonics resonators such as ribbons [8–11], disks [12–15], and cross shapes [16], due to plasmonics polaritons excitations with the photons incident from the vacuum.

Most of the previous investigations focused on graphene plasmonics with respect to the intrinsic graphene, because the nano-scale thickness of graphene (~0.335 nm) the electron properties tuning can be severely limited due to the electrons deficiency in the intrinsic graphene [17]. Recent studies have found that the graphene-thickness within ~2.68 nm can exhibit superior properties compared to the intrinsic graphene (~0.335 nm) [17]. Here, the thick graphene treated as thinned graphite with atom layer less than 10. Along with intrinsic graphene, graphene-thickness is of interest for future device applications. Although broad studies have been carried out on the physical properties of graphene-thickness, less is known about the active electron tunable plasmonics properties of graphene-thickness structures. The realization of active tunable plasmonics phenomena demonstrated in past with different noble nanostructures, such as using nano-bowtie antenna [18], nanowire tirmers [19, 20], and hole-slit nano-aperture [21] to promote the wide range of applications for sensors. Amongst them, the hollow trench geometry milled in a metal film had attracted much interest due to its unique plasmonics property based on the trench plasmonics. The electromagnetic radiation is determined at the bottom of a triangle trench milled in a metal film, which has been first predicted [22] and then experimentally revealed [23] for subwavelength confinement and moderate propagation loss. Rectangular nanotrench unique structure was also demonstrated milled in gold without graphene-thickness plasmonic indication, for realizing the single-mode channel plasmon polaritons guiding featuring subwavelength confinement and sensible propagation loss at telecom wavelengths [24]. In spite of these benefits, to achieve high tunable plasmonics at the infrared region is still challenging as rectangular trench which is composed of gold. Thus, there is a need to explore a novel way that can enhance the hybridization in gold/graphene especially in the nanoscale structure like rectangle nanotrench. Furthermore, thick graphene can be unprecedentedly tuned at infrared regime by modifying carrier concentration [4]. The use of graphene-thickness covered noble rectangular nanotrench can bring potential benefits, which can greatly enhance *e*-field at nanoscale region compared with pure metallic plasmonics nanostructures. It is believed that the plasmon properties on typical hybrid-trench geometry can be modified with different graphene thicknesses [25]. This offers a novel method for the active tuning of the *e*-field enhancement in graphene and its nanostructure. To gain accurate and effective plasmon modes, it has remained a challenge for plasmonic nanodevices and has not so well understood with graphene thicknesses based nanostructures. It enables the new opportunity for promoting the nanodevices applications for the rectangular nanotrenchs, especially for poorly fabricated nanotrench geometry with size and shape different from the designed one. However, the physics behind the graphene-covered noble system at wide infrared regime is still puzzling, especially when the graphene hybridization is actively tuned based on the graphene-thickness covered rectangle nanotrench. Therefore, it is important for understanding and exploring the plasmonic applications of the rectangular nanotrench. Besides that, it is also important to understand the plasmonic properties of graphene thicknesses with a rectangular nanotrench to explore a wide range of potential application, especially on the nanoscale level.

Here, we propose hybrid nanostructure using of finite element method (FEM), in which graphene-thicknesses are coated on rectangle dielectric nanostructure. We investigated the tunabilities in graphene electronic system; the graphene modifies the thickness with the higher impact of active tuning features. This work demonstrates polaritons in a deep metal localized resonance can couple differently with the plasmon resonances in graphene thicknesses via tuning graphene Fermi level and thickness configurations. This may offer a practical way to experimentally realize the tunable plasmonics hybridization in gold/graphene nanotrench structures. The hybrid plasmonic system described here differs mostly from the previous work [26, 27] where intrinsic graphene corresponds to alter carrier concentration in thick graphene with limited *e*-field enhancement.

We designed 2D geometry of rectangle nanotrench surrounded by the ambient medium. A perfect matching layer is set at the outer region of geometrical rectangle nanotrench. We selected the RF module from a commercial package, COMSOL, for solving the fields. The Helmholtz electromagnetic equation is used in this complete geometry for describing the near-field scattering process. Here, we carefully choose the FEM meshes as a triangle with the specific length of nanometers to assure the accuracy of the simulation results. In addition, the parameters of excited graphene with respect to the Fermi energy alterations are modeled with the surface optical conductivity that achieved by Kubo–Greenwood formula [28]:

$$\tilde{\sigma}_{\text{intra}} = \frac{2ie^2k_\mathrm{B}T}{\hbar^2\pi(\omega + i\tau_g^{-1})}\ln\left[2\cosh\left(\frac{E_F}{2k_\mathrm{B}T}\right)\right], \tag{1}$$

$$\begin{aligned}\tilde{\sigma}_{\text{inter}} &= \frac{e^2}{4\hbar}\left[\frac{1}{2} + \frac{1}{\pi}\arctan\left(\frac{\hbar\omega - 2E_F}{2k_\mathrm{B}T}\right)\right] \\ &- \frac{e^2}{4\hbar}\left[\frac{i}{2\pi}\ln\frac{(\hbar\omega + 2E_F)^2}{(\hbar\omega - 2E_F)^2 + (2k_\mathrm{B}T)^2}\right].\end{aligned} \tag{2}$$

In the equation set, T is the temperature set as 300 K (room temperature), k_B is the Boltzmann constant and E_F is the Fermi energy of excited graphene.

The schematic illustration of the hybrid plasmonic system is shown in Fig. 1a. Rectangle nanotrench milled on gold film is coated on the top of the silica substrate. Graphene with a specific thickness is coated on the top of the rectangle nanotrench structure, where W is width and D is the depth of the nanotrench, respectively. Furthermore, mechanical exfoliation adopted for fabricating thick graphene from graphite via the milling process. Bulk graphite with specific thicknesses is used here, as layered-graphene effect is considered and only layer to layer interaction is ignored. With the help of electron beam evaporation technique, a gold film is coated on a silica substrate. Then chemical vapor deposition (CVD) and the graphene transfer methods can be used to coat the graphene thicknesses on the rectangle geometry [27]. D and W are considered as a variation to modify the *e*-field properties such as enhancement and resonance wavelengths. In the current study, we have adopted tuning the Fermi level which corresponds to the 2D carrier concentration of graphene. Generally, an intraband and interband in graphene, photons with energies above $2E_F$ absorb due to transformation into the vacant states above the Fermi level. Their transformation can be analytically stated in terms of the optical conductivity of graphene. The Fermi energy (E_F) is given by

$$E_F = \hbar v_F k_F = \hbar v_F\sqrt{\pi n_{g,2\mathrm{D}}}, \tag{3}$$

where, $n_{g,\,2\mathrm{D}}$ is the carrier concentration in the two-dimensional graphene, v_F is the Fermi velocity (~1×10^6 m/s), and k_F is the Fermi wave vector. This linear dispersion indicates that charge carriers in graphene perform as massless Dirac fermions. As reported, most of the previous works consider few layer graphene to be graphene sheets with no more than few specific layers. In the current model, we treated the graphene

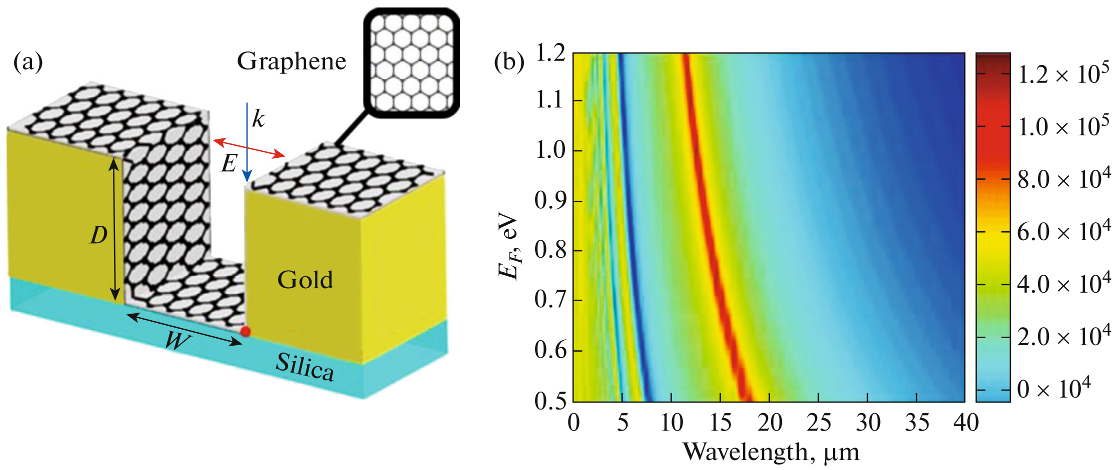

Fig 1. (a) The schematic illustration of the hybrid plasmonic system, gold film covered with intrinsic graphene (bee hive structure). The direction (k) of the incident light is perpendicular to the surface and localized e-field distributions (E) are parallel to the surface of the rectangle nanotrench. And point in the bottom right corner indicates where all results are taken. (b) Map of active tuning guideline for the wide infrared regime. It shows the tunabilities function of the rectangle nanotrench and Fermi levels with respect to the different wavelengths. The red area (in the online version of the article) shows the plasmon resonance state of rectangle trench nanostructure.

thickness as few atom layer graphite, the force of Van der Waals of different atom layers of intrinsic graphite is only considered. However, in our simulations work, it is taken that each graphene sheet has effective thickness of 0.335 nm and total corresponding thickness of few layer graphene is t = 2.68 nm. As a result, the dielectric function of few layer graphene can be acquired from its optical conductivity σ(ω) and the thickness of graphene t_g as [29–31]:

$$\varepsilon_r(\omega) = i\sigma(\omega)/(\varepsilon_0 t_g). \quad (4)$$

This is the basic reason for many novel electronic and optical properties of graphene-like large carrier mobility and allowed interband transitions from terahertz to visible frequency [32, 33]. Due to these promising electrical properties, the plasmonic response can be tuned from infrared to terahertz by increasing carrier concentration in graphene.

The map of e-field enhancement in hybrid plasmonic rectangle nanotrench structure with respect to the wavelength and graphene Fermi level is shown in Fig. 1b. Also it is taken from the right bottom corner point of the nanotrench. The red highlighted region indicates the plasmon resonance state. It is observed that the red-shift can be realized with the decreasing of Fermi level from 1.2 to 0.5 eV. It shows that this red-shift locates from 11.750 to 18.350 μm at the wide infrared frequencies. On the other hand, it demonstrates that the resonance wavelength of the rectangle nanotrench significantly increases blue-shift with Fermi levels. It can be explained as the emerged hybrid metallic resonance for a high Fermi level graphene. Furthermore, the usage of this map we adapt an active tuning guideline for the wide infrared regime. It can be helpful for tuning the plasmonic properties of design hybrid rectangle nanotrench structure via altering Fermi levels. It should be noted that the e-field enhancement in hybrid plasmon resonance needs more study especially tuning the carrier concentration at the wide infrared region.

Figure 2 demonstrates the calculated results of e-field enhancement for various thicknesses of graphene with Fermi levels alteration at the bottom of gold rectangle nanotrench with respect to the different resonance wavelengths. We can see from Fig. 2a that the e-field enhancements for synthesized nanotrench exhibit one main peak and two sub-peaks by tuning the Fermi level from 0 to 1.2 eV. The maximal e-field enhancement of 3.6×10^5 as the main peak is observed at Fermi level around 1.05 eV. The obvious tuning of the resonant wavelength of the intrinsic graphene (0.335 nm) geometry can be clearly observed in the infrared regime. We can see from Fig. 2b that the sub-peaks are emerging up, which is relative to the main peak of Fermi level of 1.1 eV. However, the e-field enhancements are totally lowered for all peaks compared to the intrinsic graphene geometry in Fig. 2a. The maximal resonance wavelength goes down, but the basic profile remains unchanged as increasing the graphene thickness from 0.335 to 0.67 nm. It can be seen from Fig. 2c that the main e-field enhancement peak approaches the highest point of thickness at 1.005 nm compared to 0.335 and 0.67 nm thickness based geometries. However, these sub-peaks are comparatively smaller than main peak of the thick graphene-covered rectangle metallic nanotrench. The maximal resonance wavelength continues to go down for the thickness 1.005 nm based geometry. We can see from Fig. 2d that the maximal e-field enhancement at

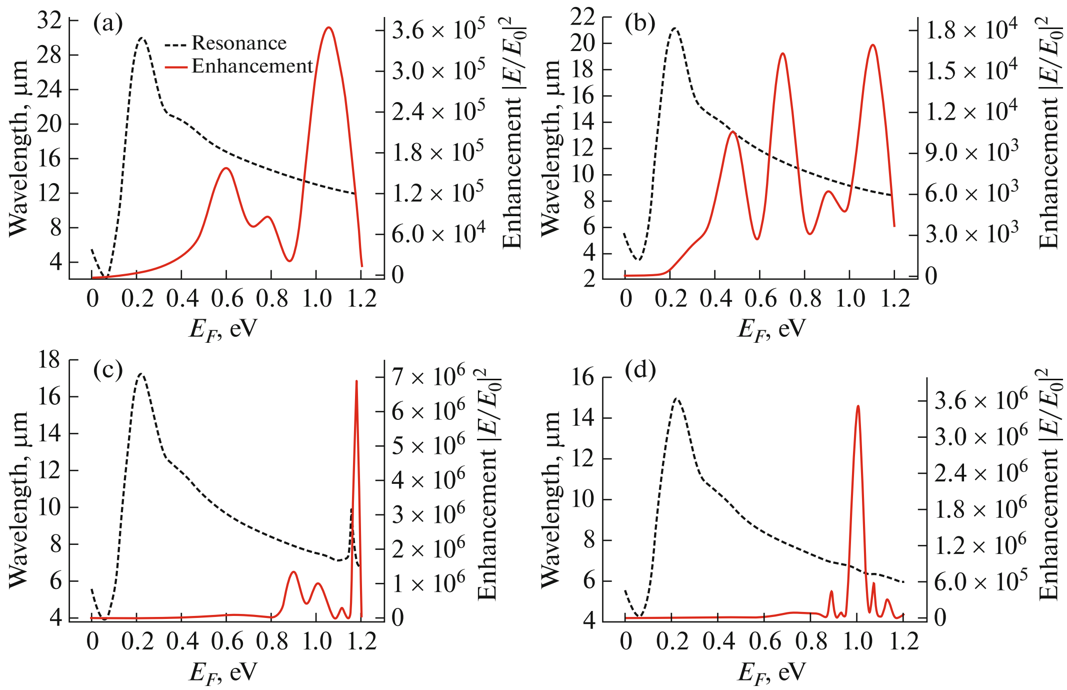

Fig. 2. Calculated results of *e*-field enhancement for thickness of (a) 0.335 nm, (b) 0.67 nm, (c) 1.005 nm, (d) 1.34 nm graphene, with Fermi levels alteration at the bottom of gold rectangle nanotrench with respect to the different resonance wavelengths.

the main peak of 3.55×10^6 is decreased compared to (6.9×10^6) 1.005 nm thick graphene.

The sub-peaks are emerging at the right side of the main peak. The result of *e*-field enhancements at the 1.34 nm geometry evidently gets weaker as compared to 1.005 nm. The above-mentioned results of the *e*-field enhancement based on gold rectangle nanotrench by tuning the Fermi level can originate from the enhanced plasmon hybridization with respect to the graphene thicknesses, which will be further explained in the following section in details.

The plasmonics hybridization from gold/graphene with tuning the carrier concentration and graphene thicknesses are shown in Fig. 3. We can see from Fig. 3a that thickness 1.005 nm can be observed with obvious *e*-field enhancement and maximum tuning increases with the decreases of the resonance, the maximal main peak of enhancement reaches to 6.9×10^6 with the 1.18 eV Fermi level in respect of 6.950 μm. Furthermore, Fig. 3b shows resonance wavelength with respect to the *e*-field enhancement corresponding to different graphene thicknesses. It can be predicted that the resonance wavelength can be obviously decreased from 12.350 to 4.550 μm as increasing the graphene thicknesses from t_1 to t_8. It can be associated with dominant role of the metallic property for gold/graphene hybridization system with enhanced thickness of graphene, where the graphene plasmonic hybridization with gold is trending to the metallic regime [34]. Moreover, it should be noted that maximal resonant wavelength positions are observed at 28.950 and 20.550 μm with graphene thickness of t_1 = 0.335 nm and t_2 = 0.67 nm, respectively. Interestingly, at t_3 = 1.005 nm, the maximal *e*-field enhancement with of 6.9×10^6 factor is obtained. It can be explained as with graphene thickness of t_3 = 1.005 nm targets can be qualified to support the strongest plasmon resonance suggesting graphene characteristic with respect to its thickness. It is reported that such properties of graphene shall be preserved till the thickness approaches 1.005 nm. Above 1.005 nm, the *e*-field enhancement decreases rapidly because of the fading of graphene characteristic during the hybridization from gold/graphene [17]. It can be clearly seen that as the graphene thicknesses within 1.005 nm have high performance, but when it exceeds to 1.675 nm, the *e*-field enhancement drops gradually, which is originated from the almost disappeared role of graphene participating in the hybridization until graphene thicknesses t_6 = 2.01 nm, t_7 = 2.345 nm, and t_8 = 2.68 nm. The results can be helpful for selecting the optimal graphene-thickness for graphene-based metallic plasmonic devices applications of nanolithography, high-sensitive SERS, sensors, and optothermal therapy.

Figure 4 shows the simulation results of gold rectangle nanotrench covered by 1.005 nm graphene thickness with respect to the modifications of the width *W* and depth *D*. By increasing the length of the rectangle nanotrench from 105 to 145 nm, the *e*-field

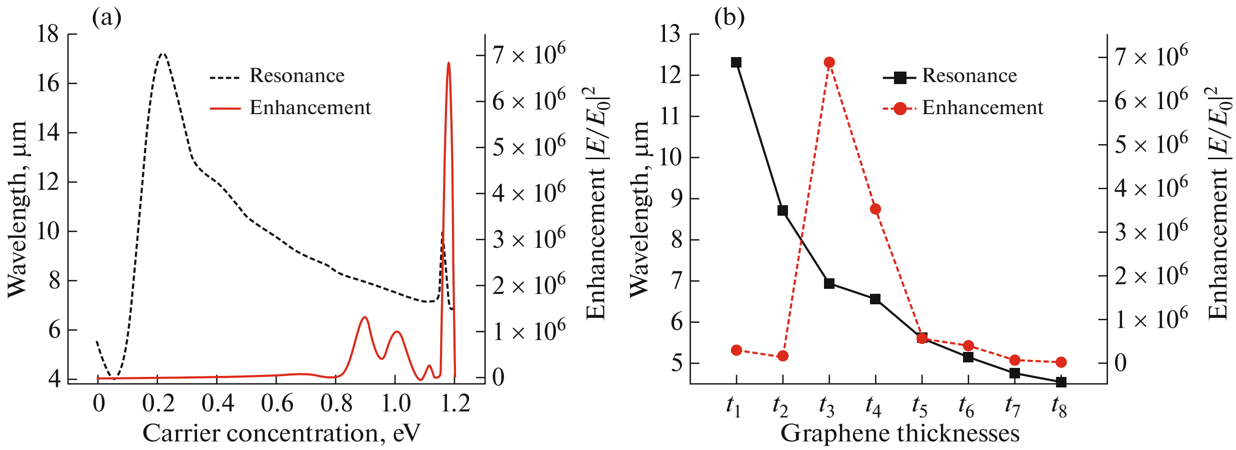

Fig. 3. (a) Maximal *e*-field enhancement realized in 1.005 nm thickness of graphene with the main peak of 6.9×10^6 at the 1.18 eV carrier concentration. (b) Graphene-thicknesses (from 0.335 to 2.68 nm) are labeled as t_1 to t_8, respectively. With respect to resonance wavelengths that correspond to *e*-field enhancements.

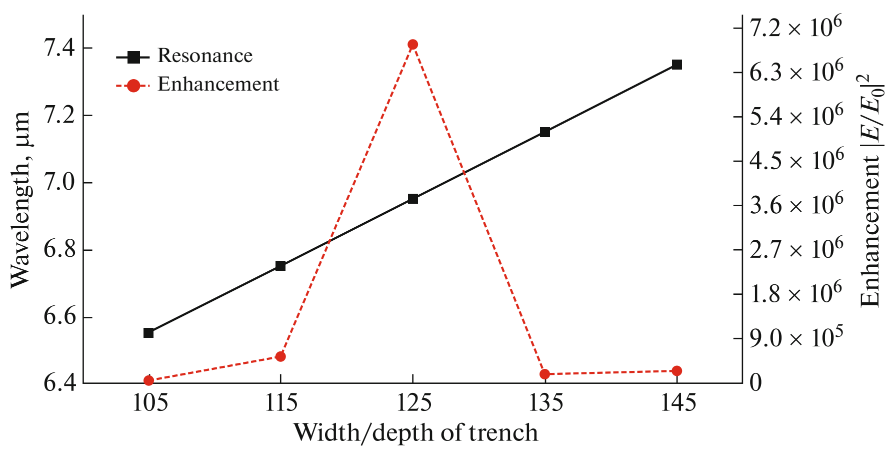

Fig. 4. Tunable plasmonics hybridization profiles of the 2D rectangle nanotrench with different width/depth are specified. Resonance wavelength and corresponding *e*-field enhancement area function of the lengths of rectangle nanotrench. These results are calculated within 1.005 nm graphene-thickness.

enhancement is evidently red-shifted from 6.550 to 7.350 μm. It exhibits stronger *e*-field enhancement of 6.9×10^6 with respect to 6.950 μm resonance wavelength at the depth of 125 nm. It can be explained as the enhanced plasmon hybridization as the length increases from 105 to 125 nm. Further, it can be observed that by increasing the length of rectangle nanotrench from 125 to 145 nm, plasmonic interaction become weaker and *e*-field enhancement declines rapidly as a result of weak *e*-field distribution in increased rectangle nanotrench width [23]. The results show that enhancement peaks can be excited and affected by the hybrid plasmon interaction in a wide wavelength range in mid-infrared from 6.550 to 7.350 μm. The plasmonic interaction can also correspond to resonance wavelength active tuning tendency with different lengths of the nanotrench. Active tunability of graphene thicknesses with the excitation of electric hybrid plasmon resonance may have possible applications for infrared band graphene photonics and optoelectronics.

In conclusion, we have theoretically investigated the tunable plasmonics properties on a rectangle nanotrench which composed of gold and thick graphene. It is found that active tunabilities can be well controlled by altering Fermi levels from 0 to 1.2 eV. It is demonstrated that rectangle nanotrench can cause obvious *e*-field enhancement of 6.9×10^6 within 1.005 nm graphene-thickness. However, after 1.005 nm *e*-field enhancements get weaker with increasing thickness of graphene, due to graphene-thicknesses and plasmon resonance off. Moreover, the *e*-field enhancement also can be tuned flexibly by changing the width W and depth D of the nanotrench.

This type of hybrid plasmonics in graphene shows very striking features including active tunabilities, efficient light-matter interactions, and electrical controllability. The tunable properties finding of rectangle nanotrench based on thicknesses of graphene nanotrench may facilitate the design of next-generation nanoscale level optoelectronic systems and sensors at wide IR range.

FUNDING

This work is supported by the National Key Research and Development Program of China under the Grant no. 2017YFB1104700, the National Science Foundation of China under the Grant nos. 51335008, 61775177, 11404254, and 61475124, the NSAF Grant no. U1630111, the Collaborative Innovation Center of Suzhou Nano Science and Technology.

CONFLICT OF INTEREST

The authors declare that they have no conflicts of interest.

REFERENCES

1. A. N. Grigorenko, M. Polini, and K. S. Novoselov, Nat. Photon. **6**, 749 (2012).
2. K. S. Novoselov, A. K. Geim, S. V. Morozov, D. Jiang, Y. Zhang, S. V. Dubonos, I. V. Grigorieva, and A. A. Firsov, Science (Washington, DC, U. S.) **306**, 666 (2004).
3. J. H. Chen, C. Jang, S. D. Xiao, M. Ishigami, and M. S. Fuhrer, Nat. Nanotechnol. **3**, 206 (2008).
4. S. V. Morozov, K. S. Novoselov, M. I. Katsnelson, F. Schedin, D. C. Elias, J. A. Jaszczak, and A. K. Geim, Phys. Rev. Lett. **100**, 016602 (2008).
5. X. Du, I. Skachko, A. Barker, and E. Y. Andrei, Nat. Nanotechnol. **3**, 491 (2008).
6. K. I. Bolotin, K. J. Sikes, Z. Jiang, M. Klima, G. Fudenberg, J. Hone, P. Kim, and H. L. Stormer, Solid State Commun. **146**, 351 (2008).
7. T. J. Booth, P. Blake, R. R. Nair, D. Jiang, E. W. Hill, U. Bangert, and A. Bleloch, Nano Lett. **8**, 2442 (2008).
8. V. W. Brar, M. S. Jang, M. Sherrott, J. J. Lopez, and H. A. Atwater, Nano Lett. **13**, 2541 (2013).
9. A. Y. Nikitin, F. Guinea, V. F. J. Garcia, and M. L. Martin, Phys. Rev. B **85**, 081405 (2012).
10. J. H. Strait, P. Nene, W. M. Chan, C. Manolatou, S. Tiwari, and F. Rana, Phys. Rev. B **87**, 241410 (2013).
11. H. Yan, T. Low, W. Zhu, Y. Wu, M. Freitag, X. Li, F. Guinea, P. Avouris, and F. Xia, Nat. Photon. **7**, 394 (2013).
12. S. Yi, M. Zhou, X. Shi, Q. Gan, J. Zi, and Z. Yu, Opt. Express **23**, 10081 (2015).
13. F. H. L. Koppens, D. E. Chang, and F. J. Garcia de Abajo, Nano Lett. **11**, 3370 (2011).
14. H. Yan, X. Li, B. Chandra, G. Tulevski, Y. Wu, M. Freitag, W. Zhu, P. Avouris, and F. Xia, Nat. Nanotechnol. **7**, 330 (2012).
15. Z. Fang, Y. Wang, A. E. Schlather, Z. Liu, P. M. Ajayan, V. F. J. Garcia, P. Nordlander, X. Zhu, and J. N. Halas, Nano Lett. **14**, 299 (2014).
16. A. Fallahi and J. P. Carrier, Phys. Rev. B **86**, 195408 (2012).
17. Y. Sui and J. Appenzeller, Nano Lett. **9**, 2973 (2009).
18. G. Du, Q. Yang, F. Chen, Y. Lu, H. Bian, and X. Hou, Appl. Phys. B **120**, 47 (2015).
19. N. Verellen, D. P. Van, C. Huang, K. Lodewijks, G. A. E. Vandenbosch, L. Lagae, and V. V. Moshchalkov, Nano Lett. **11**, 391 (2011).
20. N. Verellen, Y. Sonnefraud, H. Sobhani, F. Hao, V. V. Moshchalkov, D. P. Van, and S. A. Maier, Nano Lett. **9**, 1663 (2009).
21. N. Uddin, G. Du, F. Chen, Y. Lu, Q. Yang, H. Bian, J. Yong, and X. Hou, Plasmonics **12**, 627 (2017).
22. D. K. Gramotnev and D. F. P. Pile, Appl. Phys. Lett. **85**, 6323 (2004).
23. S. I. Bozhevolnyi, V. S. Volkov, E. Devaux, and T. W. Ebbesen, Phys. Rev. Lett. **95**, 046802 (2005).
24. S. I. Bozhevolnyi, Opt. Express **14**, 9467 (2006).
25. F. Guinea, Phys. Rev. B **75**, 235433 (2007).
26. B. Zhao, J. M. Zhao, and Z. M. Zhang, Appl. Phys. Lett. **105**, 031905 (2014).
27. X. X. Sheng, Z. Xiang, H. Yu, Q. L. Jian, L. W. Ling, and C. W. Shuang, Opt. Lett. **42**, 3052 (2017).
28. C. Semih, C. Humeyra, and O. Ekmel, Carbon **80**, 351 (2014).
29. Z. Xuetong, Z. Tian, C. Lin, H. Wei, and L. Xun, J. Lightwave Technol. **32**, 4199 (2014).
30. A. Vakil and N. Engheta, Science (Washington, DC, U. S.) **332**, 1291 (2012).
31. N. K. Emani, T. F. Chung, and X. Ni, Nano Lett. **12**, 5202 (2012).
32. K. S. Novoselov, A. K. Geim, S. V. Morozov, D. Jiang, M. Katsnelson, I. Grigorieva, S. V. Dubonos, and A. A. Firsov, Nature (London, U.K.) **438**, 197 (2005).
33. R. R. Nair, P. Blake, A. N. Grigorenko, K. S. Novoselov, T. J. Booth, T. Stauber, N. M. Peres, and A. K. Geim, Science (Washington, DC, U. S.) **320**, 1308 (2008).
34. N. K. Emani, A. V. Kildishev, V. M. Shalaev, and A. Boltasseva, Nano Photon. **4**, 214 (2015).